Robust CP-based Synchronization for DAB/DAB+ Systems over Dispersive Fading Channels

Sebastian Baumgartner, Youssef El Hajj Shehadeh, and Gangolf Hirtz

***Abstract*—In Orthogonal Frequency Division Multiplexing (OFDM) systems, symbol timing errors and frequency offsets may lead to a significant performance degradation. For this reason, it is very important to achieve a high precision time and frequency synchronization. With the absence of pilot symbols, blind synchronization algorithms using different metric functions or statistics of the received signal can be used. This paper investigates blind synchronization over dispersive fading channels by utilizing the redundant information contained in the cyclic prefix (CP). Whereas some proposed methods require channel information, this paper targets the joint estimation of the symbol timing offset, the frequency offset and the channel length.**

Starting by a previously proposed Maximum Likelihood method, we show that the approximated Log-Likelihood (LL) function exhibits a plateau and not a global maximum, leading to significant fluctuations in the estimated parameters. Yet, the symbol timing offset and the channel length characterize the position and dimensions of this plateau. Based on this finding, a novel method is developed for the joint estimation of the symbol timing offset, the frequency offset and the channel length from the approximated LL function. In addition, a second CP-based synchronization method is proposed, based on a modified timing function that targets the estimation of the parameters from the interference-free region within the cyclic prefix.

To demonstrate the performance of the proposed methods and provide a fair comparison with the most recent CP-based synchronization algorithms, Monte Carlo simulations are conducted using the OFDM-based Digital Audio Broadcasting (DAB/DAB+) system under different realistic multipath fading channel conditions. The results show that the proposed algorithms outperform considerably other algorithms in related work and are robust to varying channel conditions.

***Keywords*—OFDM, synchronization, Maximum Likelihood, timing offset, frequency offset, channel length, multipath channels.**

I. INTRODUCTION

Orthogonal Frequency Division Multiplexing (OFDM) is a commonly used technology for broadband data transmission over time and frequency selective fading channels. It is a multicarrier modulation method based on modulating each symbol on an orthogonal subcarrier. Due to its high spectral efficiency and simple detection methods, OFDM has been widely adopted in many wireless standards as LTE, WiMAX, IEEE 802.11, DAB/DAB+ , DVB-T and many others.

However, OFDM systems are sensitive to synchronization errors. The symbol timing offset (STO) describes the unknown symbol arrival time and thereby the FFT (Fast Fourier Transform) window positioning in the receiver. Therefore, accurate time synchronization is essential in an OFDM system. The carrier frequency offset (CFO) is caused by a mismatch between the carrier frequencies of the oscillators at the transmitter and the receiver, as well as Doppler-effects due to the relative motion of the transmitter and the receiver in mobile communications. Time synchronization can be performed using a specific transmitted synchronization signal (preamble), virtual subcarriers or pilot symbols within an OFDM symbol [1]–[5]. However, in OFDM systems which do not offer any predefined pilot data like Digital Audio Broadcasting (DAB/DAB+) [6], the determination of the unknown symbol timing, as well as the carrier frequency offset is an important challenging issue and therefore tackled by this paper. Interestingly, this can be achieved by leveraging the redundancy induced by the Cyclic Prefix (CP) and exploiting the correlation characteristics within an OFDM symbol [7]–[10].

Based on this principle, various blind synchronization algorithms have been proposed. In [9], the Maximum Likelihood (ML) principle has been utilized to estimate both the timing offset and the frequency offset under Additive White Gaussian Noise (AWGN) channels. This method has also been shown to perform well under flat-fading channels. However, the performance degrades in case of a frequency-selective fading channel as the algorithm results in significant fluctuations in the estimated timing offset, and tends to get an additional offset which depends on the time spread of the channel. An attempt to derive the Maximum Likelihood method over dispersive fading channels has been taken in [11], where a Likelihood function is derived based on simplified correlation characteristics. However, the method has been found to be non-robust to channel conditions as we will see in this paper. Two symbol timing synchronization algorithms over multipath fading channels were proposed in [12]. These are based on the Maximum Correlation (MC) metric and the Minimum Mean Square Error (MMSE) metric and utilize a correlation length equal to the sum of the channel length and the CP length. Another approach is proposed in [13], based on a Least Square (LS) principle for joint estimation of the symbol timing as well as the frequency offset. The paper in [7] proposes a new timing function to identify the correct STO without any information of the channel profile and channel length. The closest to this work is the idea proposed in [14]. In that paper, a new timing function is proposed and it is shown that the STO and the channel length can be both estimated from the transition characteristics of the proposed timing function.

In this paper, we first analyze the approximated Log-Likelihood (LL) function proposed in [11] showing that it exhibits a plateau over a wide range of STO and channel

Department of Electrical Engineering and Information Technology, Technische Universität Chemnitz, Germany, E-mail: {baumg, eyo, g.hirtz}@etit.tu-chemnitz.de

Manuscript received August 15, 2015, revised September 20, 2015.

length (L) values. This leads to significant fluctuations in the estimated timing offset. Yet, we show that these two parameters can be indirectly estimated from the position and dimensions of this plateau. Consequently, we propose a novel algorithm that estimates jointly the symbol timing offset and the channel length from the transition characteristics of the derived LL function. Moreover, we also propose a modified timing function which is based on seeking the interference-free region and estimating the different parameters from the samples in this region. The two methods are also extended to estimate the frequency offset.

In order to get a fair comparison between the proposed methods and the most recent CP-based synchronization algorithms, all simulations are applied to the same realistic multipath fading channel conditions and evaluated with respect to the Mean Square Error (MSE). The OFDM-based Digital Audio Broadcasting (DAB/DAB+) system [6] is used according to the channel conditions specified in [15], which are realized via a tapped-delay-line model as proposed in [16]. Through Monte Carlo simulations, the proposed algorithms are shown to outperform other methods proposed in related work and the method based on the modified timing function is shown to be robust to different multipath channels.

The rest of the paper is organized as follows: Section II describes the OFDM baseband signal received with a timing and frequency offset over a multipath fading channel. In Section III, the Log-Likelihood function for the joint estimation of the STO and the channel length is derived. After that, the proposed approaches are described in Section IV. Section V provides the simulation results for different multipath propagation channels. Finally, section VI concludes this paper.

$Notation$: Lower bold letters are used to denote vectors. The complex conjugation of a complex number is denoted by the superscript $(z)^*$, $|z|$ denotes the absolute value whereas $\mathrm{Re}\{z\}$ denotes the real part of a complex number. $E\{\cdot\}$ stands for the statistical expectation. Finally, all estimated parameters are described via $\hat{(\cdot)}$.

II. DESCRIPTION OF THE RECEIVED OFDM BASEBAND SIGNAL

At the transmitter side of an OFDM based system, the serial bitstream is first grouped and mapped onto complex constellation points $d_m(k) \in \mathbb{C}$, before being applied to an Inverse Discrete Fourier Transform (IDFT) of size N_u. The resulting m^{th} complex OFDM baseband symbol is given for every subcarrier position $n \in [0, N_u - 1]$ in the time domain as follows

$$x_m(n) = \frac{1}{\sqrt{N_u}} \sum_{k=0}^{N_u-1} d_m(k) e^{j\frac{2\pi}{N_u}kn}. \tag{1}$$

In order to prevent Inter Symbol Interference (ISI), every OFDM symbol is preceded by a cyclic prefix (guard interval) of N_g samples. One complete OFDM symbol consists therefore of $N_s = N_u + N_g$ samples. As a result, the final m^{th} transmitted time domain signal defined over $[0,\ N_s - 1]$ will be

$$s_m(n) = \begin{cases} x_m(n + N_u - N_g) & , n \in [0,\ N_g - 1] \\ x_m(n - N_g) & , n \in [N_g,\ N_s - 1] \\ 0 & , \text{otherwise.} \end{cases} \tag{2}$$

Since the CP is a copy of the last N_g samples, the following correlation properties are obtained in the transmitted symbol:

$$E\{s_m(n_1)s_m^*(n_2)\} = \begin{cases} \sigma_s^2 & , n_2 = n_1 \\ \sigma_s^2 & , n_2 = n_1 + N_u \\ 0 & , \text{otherwise} \end{cases} \tag{3}$$

where σ_s^2 is the signal power.

The obtained symbol in (2) is then transmitted over a multipath fading channel that is assumed to be quasi-stationary over M OFDM symbols. The channel impulse response can be modeled as a tapped-delay line with $(L+1)$ taps of complex attenuation factors $h(l)$. We note that for a finite channel length L, $h(l)$ = 0 for $l > L$. The guard interval length is assumed to be greater than or equal to the channel length (i.e., $N_g \geq L$), such that only a small part within the guard interval of the current m^{th} symbol is corrupted by the preceding $(m-1)^{th}$ symbol. In this case, the m^{th} received OFDM symbol depends, due to ISI, on both the m^{th} and the $(m-1)^{th}$ transmitted OFDM symbols.

Consider ε as the normalized frequency offset with respect to the subcarrier spacing and θ as the unknown symbol timing offset. The expression of the m^{th} received OFDM symbol can be written as

$$r_m(n) = e^{j\frac{2\pi n\varepsilon}{N_u}} \left(\sum_{l=0}^{L} h(l)\, s_{m-1}(n + N_s - l - \theta) + \sum_{l=0}^{L} h(l)\, s_m(n - l - \theta) \right) + \eta(n), \tag{4}$$

where $\eta \sim \mathcal{N}(0, \sigma_\eta^2)$ is a complex additive white Gaussian noise and $n = \{\theta, \theta+1, \ldots, \theta + N_u + N_g - 1\}$. The index l within the argument of $s_m(n - l - \theta)$, describes the time delay of every propagation path $l \in \{0, 1, \ldots, L\}$ with respect to the sampling time t_s of the system, i.e. $l = \lfloor \tau_l / t_s \rfloor$.

III. LIKELIHOOD FUNCTION

In this paper, the joint estimation of the symbol timing offset, the frequency offset and the channel length is investigated based on the redundancy information in the CP. Since the cyclic prefix is a copy of the last part of an OFDM symbol, the correlation characteristics between a given sample $r_m(n)$ and the corresponding separated-by-N_u sample $r_m(n+N_u)$ needs to be determined. Hereby, the expression $r_m(n+N_u)$ can be written in function of the m^{th} and the $(m+1)^{th}$ transmitted OFDM symbols as

$$r_m(n + N_u) = e^{j\frac{2\pi(n+N_u)\varepsilon}{N_u}} \left(\sum_{l=0}^{L} h(l)\, s_m(n + N_u - l - \theta) + \sum_{l=0}^{L} h(l)\, s_{m+1}(n - N_g - l - \theta) \right) + \eta(n + N_u), \tag{5}$$

where $n = \{\theta, \theta+1, \ldots, \theta+N_u+N_g-1\}$.

Due to the fact that the transmitted symbols $s_{m-1}(n)$, $s_m(n)$ and $s_{m+1}(n)$, the channel taps $h(l)$ and the noise $\eta(n)$ are mutually uncorrelated (assuming uncorrelated scattering), the auto-correlation $E\{\psi_m(n)\} = E\{r_m(n)\, r_m^*(n+N_u)\}$ between samples separated-by-N_u can be found to be

$$E\{\psi_m(n)\} = \begin{cases} \sigma_s^2\, e^{-j2\pi\varepsilon} \sum_{l=0}^{n-\theta} |h(l)|^2 & , n \in I_1 \\ \sigma_s^2\, e^{-j2\pi\varepsilon} \sum_{l=0}^{L} |h(l)|^2 & , n \in I_2 \\ \sigma_s^2\, e^{-j2\pi\varepsilon} \sum_{l=n-\theta-N_g+1}^{L} |h(l)|^2 & , n \in I_3 \\ 0 & , \text{otherw.} \end{cases} \tag{6}$$

with the intervals

$$\begin{aligned} I_1 &\equiv \{\theta, \theta+1, \ldots, \theta+L-1\} \\ I_2 &\equiv \{\theta+L, \theta+L+1, \ldots, \theta+N_g-1\} \\ I_3 &\equiv \{\theta+N_g, \theta+N_g+1, \ldots, \theta+N_g+L-1\}. \end{aligned} \tag{7}$$

On the other hand, it can be verified that $E\{|r_m(n)|^2\} = \sigma_s^2 \sum_l |h(l)|^2 \; + \sigma_\eta^2 \equiv \sigma_r^2$. For a normalized channel (i.e. $\sum_l |h(l)|^2 = 1$), we get $\sigma_r^2 = \sigma_s^2 + \sigma_\eta^2$.

According to the central limit theorem, the received sample $r_m(n)$ can be approximated for large values of N_u as a complex Gaussian random variable of variance σ_r^2; the probability density function (pdf) is given by [11]

$$f\left(r_m(n)\right) = \frac{\exp\left(-\frac{|r_m(n)|^2}{\sigma_r^2}\right)}{\pi\, \sigma_r^2}. \tag{8}$$

Consequently, the samples $r_m(n)$ and $r_m(n+N_u)$ follow a bivariate complex Gaussian distribution with a joint pdf [11]:

$$f\left(r_m(n), r_m(n+N_u)\right) = \frac{\exp\left(-\frac{|r_m(n)|^2+|r_m(n+N_u)|^2-2\rho_n \,\mathrm{Re}\left\{e^{j2\pi\varepsilon} r_m(n)\, r_m^*(n+N_u)\right\}}{\sigma_r^2(1-\rho_n^2)}\right)}{\pi^2 \left(\sigma_r^2\right)^2 (1-\rho_n^2)}, \tag{9}$$

where

$$\rho_n = \left| \frac{E\left\{r_m(n)\; r_m^*(n+N_u)\right\}}{\sqrt{E\left\{|r_m(n)|^2\right\} E\left\{|r_m(n+N_u)|^2\right\}}} \right|. \tag{10}$$

is the correlation coefficient with respect to the complex samples $r_m(n)$ and $r_m(n+N_u)$.

To derive the correlation characteristics, an observation window of length $(2N_u+N_g)$ samples needs to be considered at the receiver and therefore the likelihood function of the received vector $\mathbf{r}_m = [r_m(1), r_m(2), \ldots, r_m(2N_u+N_g)]$ is required. Yet, the multipath effects introduce correlation between the received samples which complicates the derivation of a likelihood function and a closed form expression remains an open problem. In [11], the following approximation has been considered to derive a likelihood function:

$$E\{r_m(n)\, r_m^*(n+k)\} = 0, \quad k \neq \{0, N_u\}. \tag{11}$$

Consequently, the likelihood function can be expressed as

$$\begin{aligned} \Lambda_m(\theta, L) &= f\left(\mathbf{r}_m|\theta, L\right) \\ &= \prod_{n\in I} \frac{f\left(r_m(n), r_m(n+N_u)\right)}{f\left(r_m(n)\right) f\left(r_m(n+N_u)\right)} \prod_n f\left(r_m(n)\right). \end{aligned} \tag{12}$$

where $I = I_1 \cup I_2 \cup I_3$.

The product $\prod_n f\left(r_m(n)\right)$ is thereby independent of θ and L and can be omitted. Subsequently, the likelihood function becomes

$$\Lambda_m(\theta, L) = \prod_{n\in I} \frac{f\left(r_m(n), r_m(n+N_u)\right)}{f\left(r_m(n)\right) f\left(r_m(n+N_u)\right)}. \tag{13}$$

Due to the fact that the logarithmic function is a strictly increasing function, it does not influence the following maxima search to determine the unknown parameters θ and L. Thus, the so-called Log-Likelihood (LL) function for M received OFDM symbols is finally given by

$$\Lambda(\theta, L) = \log\left(\prod_{m=1}^{M} \Lambda_m(\theta, L)\right) = \sum_{m=1}^{M} \log(\Lambda_m(\theta, L)). \tag{14}$$

Inserting (13) and the pdf specifications given by (8) and (9) into (14), one can easily get [11]

$$\Lambda(\theta, L) = \sum_{n\in I} \left\{ \frac{2\left(\rho_n \Psi(n) - \rho_n^2 \Phi(n)\right)}{\sigma_r^2\left(1-\rho_n^2\right)} - M \log\left(1-\rho_n^2\right) \right\}, \tag{15}$$

where the variables $\Psi(n)$ and $\Phi(n)$ are defined as

$$\begin{aligned} \Psi(n) &= \sum_{m=1}^{M} \mathrm{Re}\{e^{j2\pi\varepsilon} r_m(n)\, r_m^*(n+N_u)\} \\ &= \sum_{m=1}^{M} \mathrm{Re}\{e^{j2\pi\varepsilon} \psi_m(n)\}, \\ \Phi(n) &= \sum_{m=1}^{M} \frac{1}{2}\Big(|r_m(n)|^2 + |r_m(n+N_u)|^2\Big). \end{aligned} \tag{16}$$

Alternatively, (15) can now be written as a summation $\Lambda(\theta, L) = \sum_{n\in I} \Lambda_n(\theta, L)$ where

$$\Lambda_n(\theta, L) = \frac{2\left(\rho_n \Psi(n) - \rho_n^2 \Phi(n)\right)}{\sigma_r^2\left(1-\rho_n^2\right)} - M \log\left(1-\rho_n^2\right). \tag{17}$$

Before obtaining the ML estimates of θ and L, it is necessary to estimate the correlation coefficients ρ_n. These can also be estimated in a Maximum Likelihood way. By the partial derivation of the LL function with respect to ρ_n, these coefficients can be found to be the real roots of the following equation of third degree:

$$\sigma_r^2\,\rho_n^3 - \Psi(n)\,\rho_n^2 + (2\,\Phi(n) - \sigma_r^2)\,\rho_n - \Psi(n) = 0 \qquad (18)$$

The ML estimates $(\hat{\theta},\ \hat{L})$ can then be obtained by searching for the maximum of the LL function:

$$(\hat{\theta}, \hat{L}) = \arg\max_{(\theta,L)} \Lambda(\theta, L) \qquad (19)$$

Finally, the frequency offset $\hat{\varepsilon}$ can be estimated from the argument of $\psi(n) = \sum_{m=1}^{M} \psi_m(n)$ averaged over the interval I as follows:

$$\hat{\varepsilon} = -\frac{1}{2\pi} \angle \sum_{n \in I} \psi(n). \qquad (20)$$

IV. PROPOSED METHODS

A. Log-Likelihood Transition Characteristics

The approximation in (11) is only valid over AWGN or flat fading channels ($L = 0$). In this case, the LL function has a global maximum at the corresponding STO (see Fig. 1). Over a frequency-selective fading channel, the successive received samples are correlated due to the multipath effects which results in a nonzero channel-dependent correlation in (11). Therefore, the derived likelihood function is not exact and it has been found to have a plateau instead of a peak at the corresponding time offset (see Fig. 2) which results in significant fluctuations in the estimates of θ and L.

Interestingly, the position and the dimensions of the plateau depend directly on θ and L [17]. In Fig. 1 and Fig. 2, the LL function is plotted as a function of θ and L in the case $L = 0$ (flat fading channel) and $L = 9$, respectively. Graphs (a) and (b) correspond to $STO = 10$ and $STO = 20$. Comparing (a) and (b) in both figures[1], it can be observed that the position of the plateau depends directly on the symbol timing offset. On the other hand, the dimension of the plateau is influenced by the delay spread of the channel. This can be clearly seen by comparing Fig. 1 and Fig. 2. Over a flat fading channel (Fig. 1), the plateau is reduced in the plane ($L = 0$) to a single point corresponding to the STO, whereas the size of the plateau increases as the channel length increases. Moreover, we notice that the decreasing edge of the plateau corresponds to the sum: $(\theta + L)$. Thus, tracking this edge allows to get an estimate of the sum of the investigated parameters.

Based on this observation, we propose a novel algorithm for the joint estimation of the STO and the channel length using the derived LL function over dispersive multipath channels. In our algorithm (depicted in Algorithm 1), $(\hat{\tau} = \hat{\theta} + \hat{L})$ is estimated by tracking the decreasing edge of the plateau. First, an interval of $\hat{\tau}$ is defined by finding the maximum of the LL function at $L = 0$. After that, $\hat{\tau}$ is estimated by calculating the variations of the LL function around this maximum and detecting the first significant negative variation (in our implementation, the first variation that is lower than -2% is sought). The fact that the LL function behaves similarly in this area for all values of L enables to get a robust estimate $\hat{\tau}$.

[1]Note that the two curves (a) and (b) do not correspond to the exact same channel. They were generated over two different simulation runs. This explains the slight difference in the behavior of the LL function.

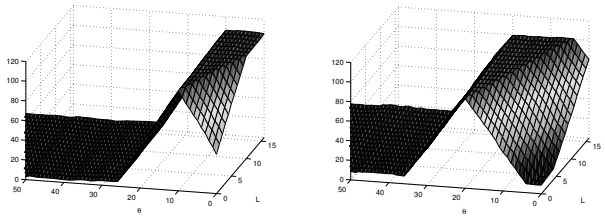

(a) $STO = 10$ (b) $STO = 20$

Fig. 1. 3D plot of the LL function for $STO = 10$ (a), $STO = 20$ (b) in the case of a flat fading channel ($L = 0$).

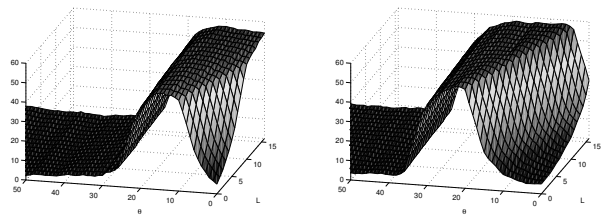

(a) $STO = 10$ (b) $STO = 20$

Fig. 2. 3D plot of the LL function for $STO = 10$ (a), $STO = 20$ (b) in the case of a multipath fading channel of length $L = 9$.

Now that $(\theta + L)$ has been estimated, it only remains to estimate one of these two parameters to obtain the other one. From Fig. 1 and Fig. 2, it can be observed that the LL function in the plane ($L = 0$) reaches its plateau at the required STO. Therefore, the estimate $\hat{\theta}$ is obtained by capturing the increasing edge of the LL function. This can simply be obtained by detecting the last significant positive

Algorithm 1 Search Algorithm for θ and L

Step 1: Find $\theta_{max} = \arg\max_\theta \Lambda(\theta, L = 0)$
Step 2: Find $\hat{\tau}$:
  $\Lambda_L(\theta) = E_L\{\Lambda(\theta, L)\}$
  for $\theta = \theta_{max}$ to $\theta_{max} + N_g - 1$ **do**
    if $\Delta\Lambda_L(\theta)/\Lambda_L(\theta) \leq -0.02$ **then**
      $\hat{\tau} = \theta$;
      $break$;
    end if
  end for
Step 3: Find $\hat{\theta}$:
  for $\theta = \hat{\tau}$ to $\hat{\tau} - N_g$ **do** {decreasing order}
    if $\Delta\Lambda(\theta, 0)/\Lambda(\theta, 0) \geq 0.02$ **then**
      $\hat{\theta} = \theta$;
      $break$;
    end if
  end for
Step 4: Find $\hat{L} = \hat{\tau} - \hat{\theta}$

variation reaching the plateau. Moreover, since $0 \leq L \leq N_g$, we first define an interval of the STO $[(\hat{\tau} - N_g),\ \hat{\tau}]$. This has been found to increase the robustness of the estimated $\hat{\theta}$ value. Finally, after obtaining $\hat{\theta}$, the estimate of the channel length can be obtained as: $\hat{L} = \hat{\tau} - \hat{\theta}$.

B. Modified Timing Function

In addition to the method based on the transition characteristics of the Log-Likelihood function, we also propose a new modified timing function that allows a high performance estimation of the timing offset and the channel length. Whereas the LL function involves a summation over the interval I, the modified timing function limits this summation to the interval I_2:

$$\tilde{\Lambda}(\theta, L) = \sum_{n \in I_2} \left\{ \frac{2\left(\rho_n \Psi(n) - \rho_n^2 \Phi(n)\right)}{\sigma_r^2 \left(1 - \rho_n^2\right)} - M \log\left(1 - \rho_n^2\right) \right\}, \tag{21}$$

Indeed, from (6) it can be seen that the intervals I_1 and I_3 involve channel effects whereas the interference-free region I_2 is independent of the channel profile. By limiting the summation to this interval, the timing function exhibits then a peak allowing an easy and accurate estimation of both the timing offset and the channel length as follows:

$$(\hat{\theta}, \hat{L}) = \arg\max_{(\theta, L)} \tilde{\Lambda}(\theta, L) \tag{22}$$

Note that (21) is a function of two variables where the interval I_2 in the summation depends on the unknown parameter L. Consequently, (21) needs to be evaluated for different values of L. The two dimensional function exhibits then a peak at the corresponding values of θ and L.

The frequency offset can also be estimated similar to (20) but by limiting the summation to the interference-free region I_2:

$$\hat{\varepsilon} = -\frac{1}{2\pi} \angle \sum_{n \in I_2} \psi(n). \tag{23}$$

V. Simulation results and discussions

In order to demonstrate the performance of the proposed methods and compare them with the most recent blind synchronization algorithms, all procedures are applied to the OFDM based Digital Audio Broadcasting (DAB/DAB+) system in transmission mode III according to the specifications in [6]. In this mode every OFDM symbol consists of 192 active subcarriers which are modulated via a $\pi/4$-DQPSK, a FFT size of $N_u = 256$ and a guard interval of $N_g = 63$ samples, respectively. The channel is specified according to the norm given in [15], which is based on the COST-207 channel specification [18]. The Typical Urban (TU) and Bad Urban (BU) channel models are adopted for the simulations. The corresponding channel-tap powers and delays as well as Doppler profiles are summarized in Table I. The multipath channels are thereby realized via a tapped-delay-line model according to [16] and are fixed in each OFDM symbol but independent from one run to another within 10^3 Monte Carlo trials. Without loss of generality, in every simulation run the symbol timing is fixed to $\theta = 5$ samples and the frequency offset ε is $1/3$ of the subcarrier spacing, i.e. 2.667 kHz. Unless otherwise stated, $M = 5$ OFDM symbols are considered. The results are evaluated in terms of the probability of lock-in[2] ($P(\hat{\theta} = \theta)$) +, the Normalized (with respect to N_u^2) Mean Square Error (NMSE) between the estimated and real STO, and the NMSE of the frequency offset for different signal-to-noise ratios (SNR).

TABLE I
Channel parameters for the simulation

(a) Typical Urban channel according to [15], [18]

Parameters	Values
Tap delays [μs]	$[0, 0.2, 0.6, 1.6, 2.4, 5.0]$
Tap powers [dB]	$[-3, 0, -2, -6, -8, -10]$
Doppler profile	[Jakes,Jakes,Gauß1,Gauß1,Gauß2,Gauß2]

(b) Bad Urban channel according to [15], [18]

Parameters	Values
Tap delays [μs]	$[0, 0.4, 1.0, 1.6, 5.0, 6.6]$
Tap powers [dB]	$[-3, 0, -3, -5, -2, -4]$
Doppler profile	[Jakes,Jakes,Gauß1,Gauß1,Gauß2,Gauß2]

In the following, the modified ML method in AWGN and flat-fading channels [9], [19] is specified by (MLA) under the assumption of an ideal knowledge of the correlation coefficient according to (10). The Maximum Correlation procedure of [12] is denoted by (MC), and the Minimum Mean Square Error algorithm is denoted by (MMSE). The algorithm based on a new timing function proposed in [14] is denoted by (NTF). The ML algorithm over dispersive channels [11] according to (19) is denoted as (MLD). Recall that this algorithm exhibits significant fluctuations in the estimated STO, resulting in a high error floor. Finally, the proposed method based on the transition characteristics of the LL function is denoted by (LLTC) and the method based on the modified timing function (21) is denoted as (ML-I2).

Fig. 3 shows the simulation results ((a) Probability of Lock-in, (b) NMSE of STO, and (c) NMSE of CFO) in case of a Typical Urban channel whereas Fig. 4 shows the results for a Bad Urban channel model [15], [18]. Observing Fig. $3(a)$ and Fig. $4(a)$, it can be clearly noted that the proposed algorithms outperform significantly the other algorithms in terms of the probability of lock-in. In contrary to other algorithms which exhibit an error floor, the performance of the proposed algorithms increase with the SNR. This can also be seen in the NMSE curves of the STO in Fig. $3(b)$ and Fig $4(b)$. Moreover, it is interesting to note that the (ML-I2) method is more robust to channel conditions than (LLTC) as it shows high performance over both channel models whereas the performance of (LLTC)

[2]Note that this definition is different to some works where the probability of lock-in is evaluated with respect to the interference free region, where the correction of the remaining rotation is left to the equalizer.

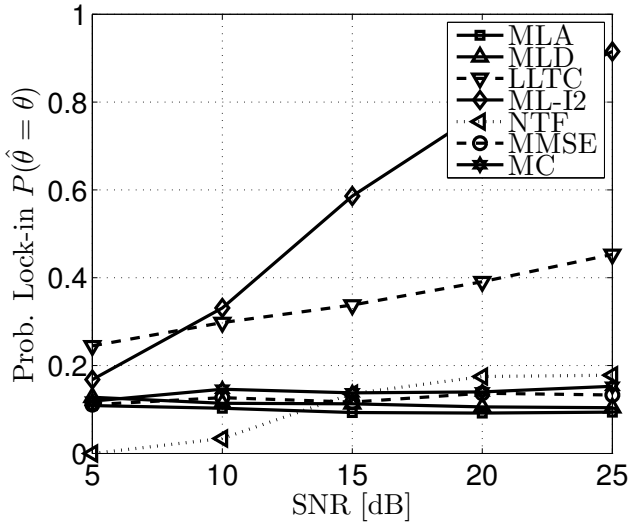

(a) Probability of Lock-in as a function of SNR

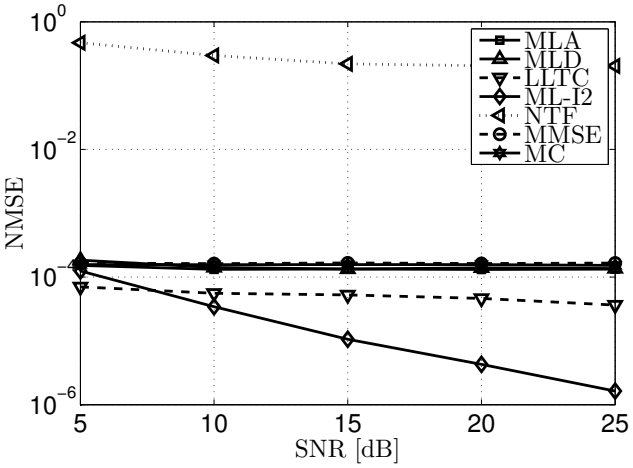

(b) NMSE of the STO as a function of SNR

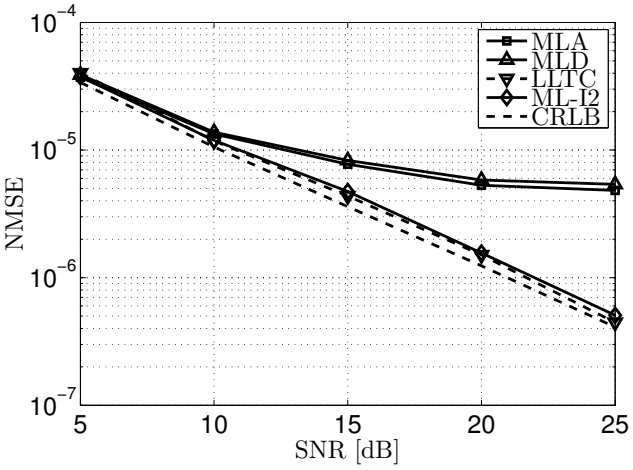

(c) NMSE of the CFO as a function of SNR

Fig. 3. Simulation results in case of a Typical Urban channel [15], [18]

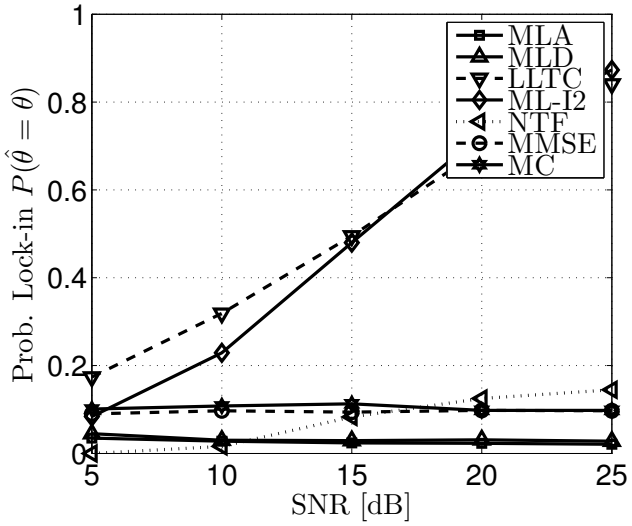

(a) Probability of Lock-in as a function of SNR

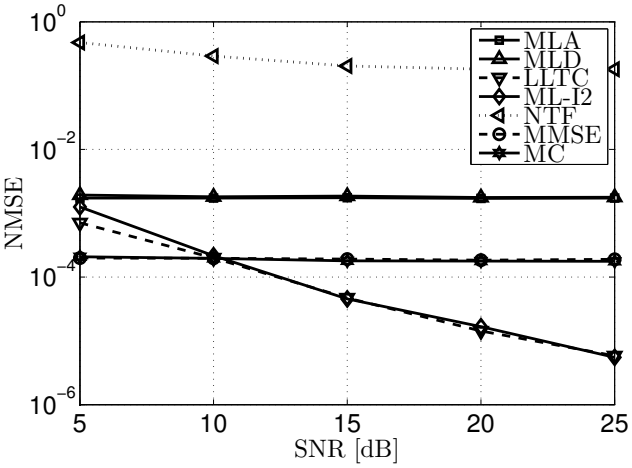

(b) NMSE of the STO as a function of SNR

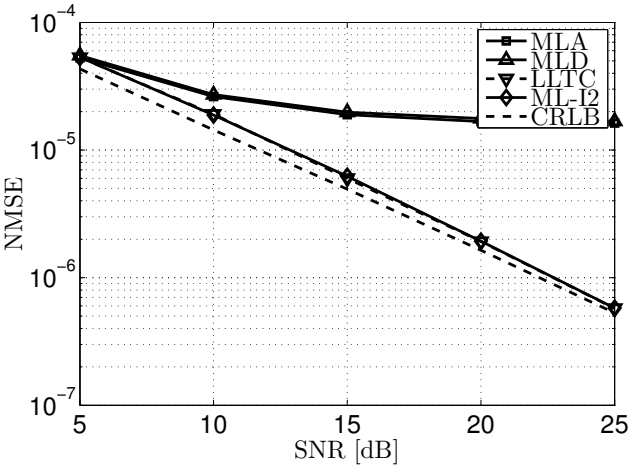

(c) NMSE of the CFO as a function of SNR

Fig. 4. Simulation results in case of a Bad Urban channel [15], [18]

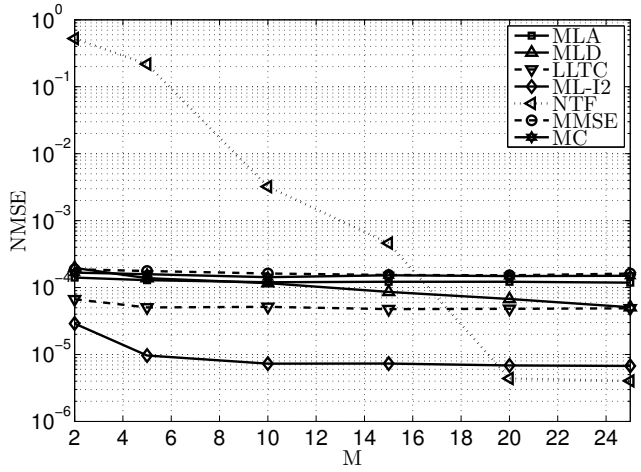

(a) NMSE of the STO as a function of M

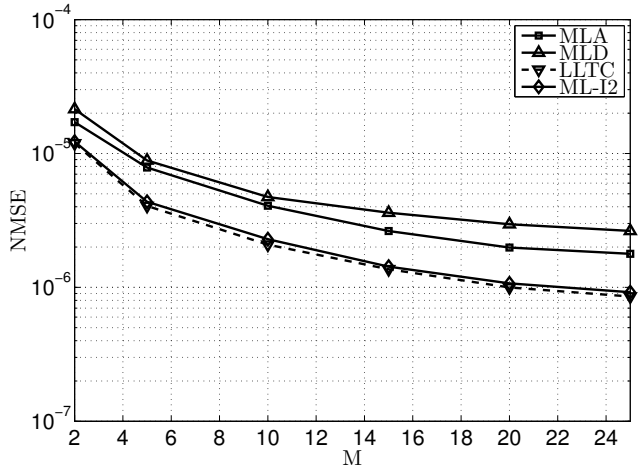

(b) NMSE of the CFO as a function M

Fig. 5. Simulation results in case of a Typical Urban channel [15], [18] for SNR= 15 dB

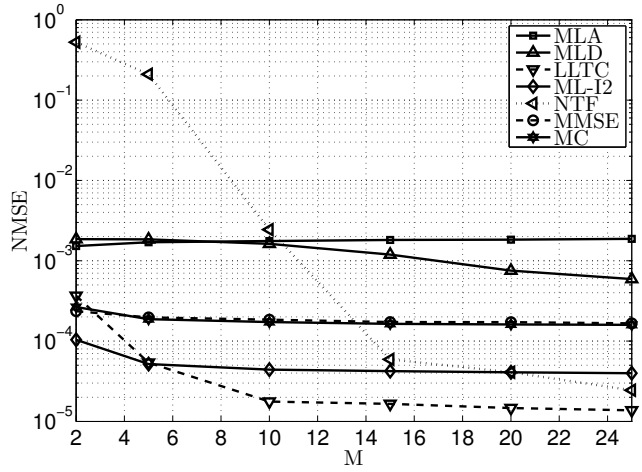

(a) NMSE of the STO as a function of M

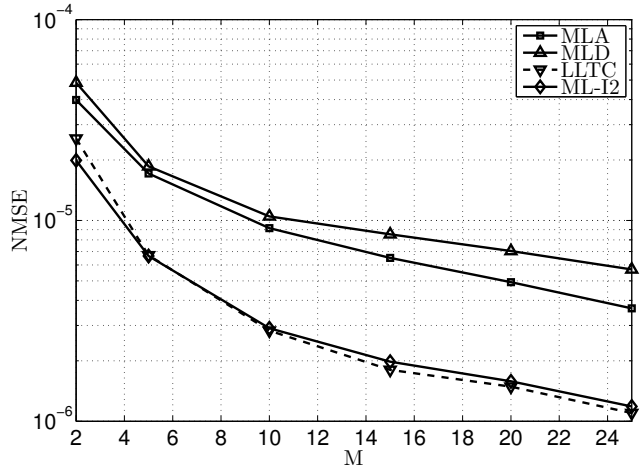

(b) NMSE of the CFO as a function M

Fig. 6. Simulation results in case of a Bad Urban channel [15], [18] for SNR= 15 dB

is much less over the Typical Urban channel.

The simulation results for the frequency offset are shown in Fig. $3(c)$ and Fig. $4(c)$, for the Typical Urban and Bad Urban channels, respectively. The results of the MLD and MLA methods are similar to each other and do not show much improvement with a higher SNR. On the other hand, the proposed methods show very high performance as the MSE of the frequency offset is close to the Cramér-Rao lower bound (CRLB), which is derived in [11].

Finally, Fig. 5 and Fig. 6 show the results of the STO mean squared error and the CFO mean squared error as a function of the number of OFDM symbols M for an SNR of 15 dB over the Typical Urban and the Bad Urban channels, respectively. In terms of STO estimation (Fig. $5(a)$ and Fig. $6(a)$), the proposed algorithms outperform all other algorithms for most values of M and over both channels. The (LLTC) method shows again that its performance depends on the channel profile. While its performance is worse than (ML-I2) over the Typical Urban channel model, it shows a better performance over the Bad Urban channel. It is interesting to see that the (NTF) method works well for high values of M (M>20) and outperforms slightly (ML-I2) over the Typical Urban channel. However, a high value of M results in higher computational complexity and requires bigger buffer sizes. Due to the good performance for a small parameter M, the proposed methods can be used in the acquisition as well as the tracking phase. As for CFO estimation (Fig. $5(b)$ and Fig. $6(b)$), the proposed algorithms show a similar performance and outperform the (MLA) and (MLD) methods significantly, especially over the Bad Urban channel.

VI. CONCLUSION

In this paper, blind synchronization based on the cyclic prefix in OFDM systems has been investigated. A previously proposed Maximum Likelihood method for the joint estimation of the symbol timing offset and the channel length over dispersive channels has been revisited. It has been shown that the method yields significant fluctuations in the estimation of the symbol timing offset. This is due to a simplification considered in the derivation of the Log-Likelihood method

which was found to exhibit a plateau instead of a global maximum.

Observing that the dimensions and the position of this plateau depend directly on the values of the STO and the channel length, we have proposed a novel CP-based synchronization method. The method estimates the symbol timing offset and the channel length from the size and position of the plateau of the obtained LL function. Moreover, observing that the interference-free region within the cyclic prefix is characterized by channel-profile independent correlation characteristics, a modified timing function is also proposed. This function has been found to exhibit a global maximum allowing a simple estimation of the STO and channel length. In addition, both methods were extended with frequency offset estimation by seeking the argument of the correlation function during the interference-free region.

Simulation results based on the DAB/DAB+ system specifications over realistic channel models have verified the high performance of the proposed methods. In contrast to other CP-based synchronization algorithms, the proposed method based on the modified timing function has been found to be robust to channel conditions showing a high accuracy in the estimation of the timing and frequency offsets over different channel models.

REFERENCES

[1] L. Nasraoui, L. N. Atallah, and M. Siala, "Performance evaluation of an efficient reduced-complexity time synchronization approach for OFDM systems," *annals of telecommunications-annales des télécommunications*, vol. 69, no. 5-6, pp. 321–330, 2014.

[2] B. Shoba, T. Thamizhilakiya, and K. Jayanthi, "A Robust Training-Symbol Based Timing Synchronization for OFDM Systems," *Digital Signal Processing*, vol. 5, no. 7, pp. 243–251, 2013.

[3] H.-T. Hsieh and W.-R. Wu, "Maximum Likelihood Timing and Carrier Frequency Offset Estimation for OFDM Systems With Periodic Preambles," *IEEE Transactions on Vehicular Technology*, vol. 58, no. 8, pp. 4224–4237, Oct 2009.

[4] J. Zhang and M. Wang, "The Improvement of OFDM Symbol Timing Synchronization Based on Continuous Pilot," *Journal of Computational Information Systems*, vol. 9, no. 24, pp. 10 095–10 102, 2013.

[5] X. Ma, C. Tepedelenlioglu, G. B. Giannakis, and S. Barbarossa, "Non-Data-Aided Carrier Offset Estimators for OFDM With Null Subcarriers: Identifiability, Algorithms, and Performance," *IEEE Journal on selected areas in communications*, vol. 19, pp. 2504–2515, 2001.

[6] European Telecommunications Standards Institute (ETSI), "ETSI EN 300 401 V1.4.1: Radio Broadcasting Systems; Digital Audio Broadcasting (DAB) to mobile, portable and fixed receivers," January 2006.

[7] S. Ma, X. Pan, G. Yang, and T. Ng, "Blind Symbol Synchronization Based on Cyclic Prefix for OFDM Systems," *IEEE Transaction on Vehicular Technology*, vol. 58, pp. 1746–1751, 2009.

[8] B. Ai, Z.-X. Yang, C.-Y. Pan, J. hua Ge, Y. Wang, and Z. Lu, "On the synchronization techniques for wireless OFDM systems," *IEEE Transactions on Broadcasting*, vol. 52, no. 2, pp. 236–244, June 2006.

[9] J. van de Beek, M. Sandell, and P. O. Borjesson, "ML Estimation of Time and Frequency Offset in OFDM Systems," *IEEE Transaction on Signal Processing*, vol. 45, pp. 1800–1805, 1997.

[10] M. J. Canet, V. Almenar, S. J. Flores, and J. Valls, "Low Complexity Time Synchronization Algorithm for OFDM Systems with Repetitive Preambles," *Journal of Signal Processing Systems*, vol. 68, no. 3, 2012.

[11] W. L. Chin, "ML Estimation of Timing and Frequency Offsets Using Distinctive Correlation Characteristics of OFDM Signals Over Dispersive Fading Channels," *IEEE Transaction on Vehicular Technology*, vol. 11, pp. 444–456, 2011.

[12] D. Lee and K. Cheun, "Coarse Symbol Synchronization Algorithms for OFDM Systems in Multipath Channels," *IEEE Communication Letters*, vol. 6, pp. 446–448, 2002.

[13] T. Fusco and M. Tanda, "Blind Synchronization for OFDM Systems in Multipath Channels," *IEEE Transaction on Wireless Communications*, vol. 8, pp. 1340–1348, 2009.

[14] X. Liu, K. Pan, Y. Zuo, and J. Chen, "Blind Symbol Synchronization for OFDM Systems in Multipath Fading Channels," *International Conference on Wireless Communications, Networking and Mobile Computing (WICOM)*, vol. 58, pp. 1746–1751, 2010.

[15] DIN Deutsches Institut für Normung e.V., "Characteristics of DAB Receivers; German Version EN 50248:2001," April 2002.

[16] S. Baumgartner, G. Hirtz, and A. Apitzsch, "Methods for Simulation of the Wireless Propagation Channel for DAB/DAB+/DMB-SDR-Receivers," *IEEE Eurocon 2013*, pp. 138–145, 2013.

[17] Y. E. H. Shehadeh, S. Baumgartner, and G. Hirtz, "A Robust Blind Time Synchronization Method in OFDM Systems over Multipath Fading Channels," in *European Wireless*, May 2015.

[18] M. Failli (Chairman), COST 207 Management Committee of the European Commission, *COST 207: Digital land mobile radio communications*. European Commission, December 1989.

[19] S. Baumgartner, Y. E. H. Shehadeh, and G. Hirtz, "Performance Evaluation of Frequency and Symbol Timing Offset Estimation Methods for DAB/DAB+ Receivers under Multipath Fading Channels," in *The 22nd International Conference on Software, Telecommunications and Computer Networks - SoftCOM*, September 2014.

Sebastian Baumgartner was born in Tirschenreuth, Germany in 1982. He received his Dipl. Math. degree in applied mathematics from the University of applied science in Regensburg, Germany in 2006, In 2011, he received his Dipl.-Ing. degree in electrical engineering from the University of Technology in Chemnitz, Germany, where he is currently working toward the Ph.D. degree in the field of blind synchronization of OFDM based systems. His research interests include stochastical signal processing and blind parameter estimation in multicarrier communication systems.

Youssef El Hajj Shehadeh is currently a postdoctoral researcher at the Chair of Digital Signal Processing and Circuit Design, Chemnitz University of Technology, Germany. He received the PhD degree in 2013 from the institute of Applied Computer Science/Telematics group at the University of Goettingen, Germany. He holds an engineering diploma degree (2009) in Telecommunications from the Lebanese University of Beirut, Lebanon and a master of research degree (2009) in "Digital Telecommunication Systems" from Telecom Paristech (ENST Paris). His research interests vary between digital communications, resource allocation and medium access techniques, and security in wireless networks mainly on the physical layer level.

Gangolf Hirtz has many years of industrial experience in the areas of consumer and automotive electronics. Since 2008, Prof. Dr.-Ing. Gangolf Hirtz heads the chair of Digital Signal Processing and Circuit Design at Chemnitz University of Technology. His current research interests include Camerabased behavior detection of elderly and wireless communications.